HHS Public Access

Author manuscript

*Angew Chem Int Ed Engl*. Author manuscript; available in PMC 2021 May 04.

Published in final edited form as:

*Angew Chem Int Ed Engl*. 2020 May 04; 59(19): 7450–7455. doi:10.1002/anie.202001516.

# An Excimer Clamp for Measuring Damaged Base Excision by the DNA Repair Enzyme NTH1

**Yong Woong Jun**[a], **David L. Wilson**[a], **Anna M. Kietrys**[a], **Elizabeth R. Lotsof**[b], **Savannah G. Conlon**[b], **Sheila S. David**[b], **Eric T. Kool**[a]

[a]Department of Chemistry, Stanford University, Stanford, CA 94305

[b]Department of Chemistry, University of California, Davis, Davis, CA 95616

## Abstract

Direct measurement of DNA repair enzyme activities is important both for basic study of cellular repair pathways as well as for potential new translational applications in their associated diseases. NTH1, a major glycosylase targeting oxidized pyrimidines, prevents mutations arising from this damage, and the regulation of NTH1 activity is important in resisting oxidative stress and in suppressing tumor formation. Here we describe a novel molecular strategy for the direct detection of damaged DNA base excision activity by a ratiometric fluorescence change. This strategy utilizes glycosylation-induced excimer formation of pyrenes, and modified DNA probes incorporating two pyrene deoxynucleotides and a damaged base enable the direct, real-time detection of NTH1 activity *in vitro* and in cellular lysates. The probe design was also applied in screening for potential NTH1 inhibitors, leading to identification of a new small-molecule inhibitor with sub-micromolar potency.

## Graphical Abstract

kool@stanford.edu.
Institute and/or researcher Twitter username: @koolchemistry

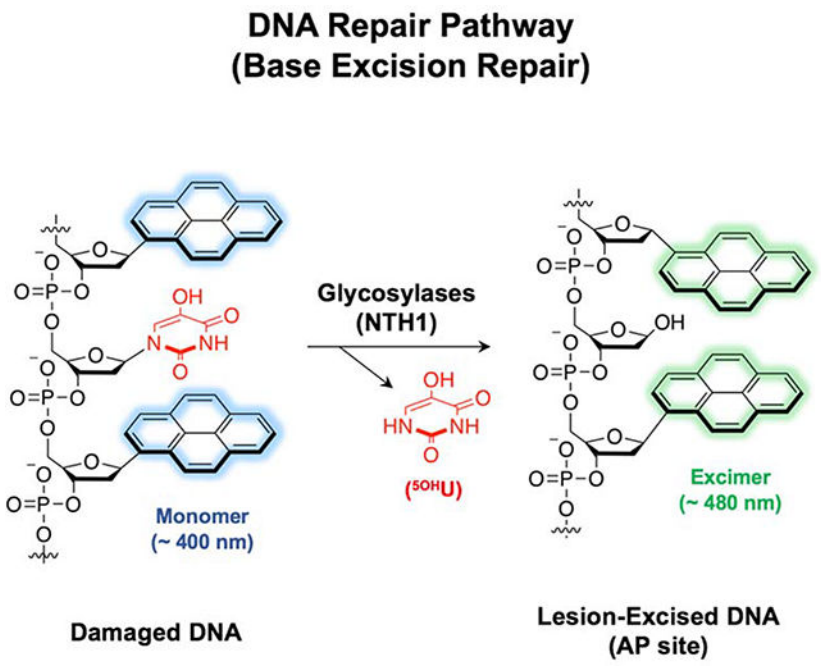


Direct measurement of NTH1 glycosylase activity is of interest for the study of this DNA repair pathway and related diseases. A DNA probe design for glycosylase activity is reported which relies on a “clamp” of pyrenes and shows a robust ratiometric response. Assays are developed for measuring activity of NTH1 both *in vitro* and in cell lysates, and are further utilized for high-throughput screening to find a selective inhibitor of NTH1.

**Keywords**

DNA Repair; NTH1; Glycosylases; Base Excision Repair (BER); Excimer Formation

The integrity of genomic DNA is continuously challenged by reactive oxygen species (ROS) that are endogenously generated through cellular oxidative metabolism.[1] The frequency of DNA damage events such as DNA base oxidation, DNA base loss creating apurinic/apyrimidinic (AP) sites, and DNA strand breaks has been estimated at over 10,000 events per cell per day.[2] If unrepaired, the accumulated DNA damage has the capacity to result in permanent genetic change or activation of cell death responses resulting in mutagenesis, carcinogenesis, and neurodegenerative pathologies.[3]

Base excision repair (BER) constitutes a class of biochemical pathways responsible for the removal of DNA lesions and coordinating their replacement with the correct undamaged base, and thus is essential for the maintenance of genomic stability.[4] The critical first step of BER consists of the recognition and removal of the damaged base by a damage-specific DNA glycosylase.[5] Among 11 BER glycosylases identified thus far in human cells, the major DNA glycosylases that target oxidized DNA bases include 8-oxoguanine DNA glycosylase (OGG1), endonuclease III-like protein 1 (NTH1), and endonuclease VIII-like proteins (NEILs). The abasic site generated from the hydrolysis of the N-glycosyl bonds by

the glycosylases is subsequently cleaved by an AP lyase activity (in some cases, associated within the same glycosylases) or by a separate AP endonuclease activity. In most circumstances, the one-base gap in the cleaved DNA strand is then filled in by a DNA polymerase and ligated by a DNA ligase, to restore the original genetic information.[6]

NTH1, a DNA glycosylase with associated AP lyase activity, constitutively recognizes oxidized pyrimidines, including 5-hydroxy-uracil ($^{5OH}$U), 5-hydroxy-cytosine ($^{5OH}$C), and thymine glycol (Tg) (Figure 1a).[7] Among these several types of oxidized pyrimidines, $^{5OH}$U in DNA has been reported to be abundantly produced from C and causes C→T mutations as a human polymerase (Polι) bypasses $^{5OH}$U, preferentially incorporating T opposite the lesion.[8] Small interfering RNA (siRNA) depletion of *nth1* mRNA in TK6 cells has been shown to decrease cellular resistance to hydrogen peroxide treatment, while higher cellular resistance was observed when NTH1 was overexpressed.[9] Furthermore, the repair of oxidative DNA damage in *nth1* knockout mouse embryonic fibroblasts has been shown to be significantly impaired,[10] and reduced expression levels of NTH1 have been observed in prostate cancer cells[11] and in patients with gastric cancer.[12] These findings suggest that the regulation of NTH1 activity is important in the cellular response to oxidative stress and in suppressing tumor formation.

Despite the biomedical significance of this enzyme, the development of direct and reliable methods for measuring the repair activity of NTH1 remains challenging.[1, 3] For instance, immunohisto-chemistry requires multiple steps of sample preparation, staining, and washing, and measures protein quantity rather than enzyme activity. Given that the enzyme is known to undergo posttranslational modifications that alter the BER activity,[1, 13] the protein quantity may not correlate directly with activity.[14] *In vitro* assays of NTH1 enzyme activity typically involve gel electrophoresis, followed by the quantification of cleaved DNA products, which is laborious and indirect.[15] The measurement of NTH1 activity in biological samples such as cell lysates, tissue extracts, or live cells is even more challenging. While two fluorescence reporters have been developed for NTH1, both reporters involve secondary reactions to yield fluorescence signal, and thus are not directly linked to the glycosylase reaction alone.[16] Indirect output probes are also likely to have limited utility in biological environments owing to the requirement of multiple steps for signal generation. Recently, fluorescent DNA probes for the direct analysis of other DNA repair activities have been developed based on the fluorescence quenching effect of neighboring bases.[17] Such methods, while effective for certain enzymes, are limited to damaged base/fluorophore combinations that yield effective quenching. To date, there has been no report of the direct detection of the DNA base excision activity of NTH1.

Here we describe a novel molecular strategy for design of fluorogenic probes for DNA base excision repair. Because the approach does not rely on quenching by the damaged base, it is potentially generalizable to multiple types of DNA damage. Additionally, this strategy offers a ratiometric fluorescence response which enables reliable measurement in complex environments such as biological samples by a built-in self-referencing capability.[18] The new probe design, designated **GPE** (glycosylase induced pyrene excimer formation), was developed for NTH1 activity and employed for measuring this activity in biological samples. We further show that **GPE** probes can be used in probe-coupled assays to identify new leads

for small-molecule NTH1 inhibitors and activators, which may themselves be useful in analysis of the overlapping pathways involved in oxidized pyrimidine repair.

Our design of fluorogenic probes for NTH1 relies on the excimer formation of two pyrene nucleobase analogues[19] that are initially separated when a damaged base exists between them (Figure 1c). Excision of the damaged base by a glycosylase, creating an AP site between the two pyrenes, potentially enables the pyrenes to interact to form an excimer. The initial probe oligo-nucleotide with the damaged base was expected to exhibit blue fluorescence (~400 nm) from the separate pyrene monomers, and after the excision of the damaged base, an excimer would be expected to fluoresce in green wavelengths (~480 nm) from pyrene excimer formation.[20] The probe design includes double-stranded hairpin oligonucleotide structure, as well as a sensing part consisting of two pyrene deoxyribosides with the damaged base between in the hairpin stem (Figure 1b). The double-stranded architecture was chosen based on reports that NTH1 is only active with duplex DNA.[21] A highly stabilizing GAA loop was chosen to enhance folding stability in short sequences.[22] In the complementary strand of the sensing part, the pyrenes were paired opposite abasic dSpacers, enabling the pyrenes to occupy similar space as canonical base pairs without strong helical distortion;[23] pyrene-abasic pairs have been shown to exhibit stability similar to that of A-T base pairs.[23b] The damaged base employed in the probe ($^{5OH}$U) was paired with G since $^{5OH}$U is usually derived from C and forms the most stable base pair with G (SI Table S1).[24]

To test the design concept, three oligonucleotides were synthesized using phosphoramidite chemistry with different bases between pyrenes (Figure 2a); C (**GPE_Intact**, a control lacking damage), $^{5OH}$U (**GPE_Damaged**, which is expected to be an enzyme excision substrate), and dSpacer (**GPE_Excised**, a mimic of the expected base excision product).[19, 25] While fluorescence spectra of **GPE_Intact** and **GPE_Damaged** showed nearly identical patterns with monomer (400 nm) and excimer (480 nm) signals, that of **GPE_Excised** showed strongly enhanced excimer fluorescence with minimal residual monomer signal (Figure 2b). Increasing the temperature of **GPE_Damaged** resulted in the melting of the DNA oligonucleotide, which also favors the formation of excimer (SI Figure S1), presumably by flipping the damaged base out of the helix. The results suggest that the structural arrangement of the pyrenes with the damaged base is central to its responsive fluorescence properties.

With human NTH1 enzyme (hNTH1), **GPE_Damaged** yielded a monomer/excimer ratio increase over the period of an hour, and higher concentrations of hNTH1 resulted in greater changes in the ratio (Figure 2c). In control experiments, the ratio of **GPE_Intact** treated with hNTH1 remained unchanged, which is the same result as that of **GPE_Damaged** in the absence of hNTH1. The cleavage of the damaged base by hNTH1 was further confirmed by MALDI-TOF analysis (SI Figure S9). Since pyrene fluorescence can be strongly affected by neighboring DNA bases,[26] we prepared **GPE** probes with four different neighboring base combinations (Figure 2a, 2d). **GPE(GCCG)**, which showed the most promising signal change among those tested, was subjected to substrate-length preference evaluation by changing the length of its stem from 7 to 19 bp (Figure 2a, 2e). Given that the activity of hNTH1 toward **GPE7** and **GPE19** were significantly lower than that of **GPE11** and **GPE15**,

we concluded that hNTH1 prefers the length of stems in the range of 11–15 base pairs in this context. Interestingly, the opimized DNA probe, **GPE11**, shows a $K_M$ value 0.71 $\mu$M with hNTH1, in the same range of the reported $K_M$ value of hNTH1 (0.45–1.35 $\mu$M) toward the same damaged base ($^{5OH}$U) in a fully natural DNA context (SI Figure S10).[27] This establishes that the adjacent pyrene-abasic pairs in **GPE11** are not strongly disruptive to the helical structure, nor to hNTH1 enzyme-DNA interactions.

To test the utility of **GPE11** in differentiating activity levels of NTH1 in cells, the probe was modified as a nuclease-protected version (**GPE11np**) by substituting two deoxyribonucleotides with 2'-*O*-methyl nucleotides at both 3' and 5' termini, and with a hexaethylene glycol linker in place of the GAA loop (Figure 3c, SI Table S1).[28] Similar end-modifications have proven to be effective in lowering background signals from nuclease cleavage in other DNA-based enzyme probes.[29] Tests with purified enzyme confirmed that the modification had little measurable effect on the response toward NTH1 (SI Figure S2). **GPE11np** was then tested with lysates from HeLa cells in a 384-well plate-reader over an extended period at 37 °C (Figure 3d). The excimer fluorescence of **GPE11np** was observed to increase over 10 h, responding to enzymatic activity from cell lysates containing endogenous NTH1. Considering that $^{5OH}$U is a substrate of multiple glycosylases (most notably NTH1, NEIL, and SMUG1), it was anticipated that fluorescence enhancement of **GPE11np** in lysate is not exclusively dependent on NTH1.[30] To estimate the portion of NTH1 activity from the entire $^{5OH}$U excision activity, we prepared NTH1 knock-down cellular lysate by transfecting a small interfering RNA (siRNA) shown previously to effectively ablate *nth1* mRNA (Figure 3a).[31] Western blot results confirmed that NTH1 protein was knocked down (to less than 3.5% of native levels) after 48 h of incubation of siNTH1 (Figure 3b). Application of the **GPE11np** probe in this *nth1* knock-down lysate resulted in a ca. 30% decrease in fluorescence enhancement compared to the control cell lysate, which implies that approximately 30% of $^{5OH}$U BER processing is performed by NTH1 in HeLa cells (Figure 3d).

Given the biomedical connections of NTH1 to cancer and other diseases, it will be useful in the future to develop small-molecule modulator compounds that can probe its biological roles in cell and animal models. Inhibitors of glycosylases can provide insight into their roles in cellular repair pathways, and can be especially useful when overlapping pathways exist, such as occurs for NTH1. In general, DNA repair inhibitors are clinically important in cancer treatment;[32] cancer cells maintain the viability in high concentration of ROS through elevated DNA repair activity, and inhibiting DNA repair pathways can confer synthetic lethality to cancer cells.[33] Using **GPE** probes of NTH1 activity, we developed an *in vitro* fluorescence assay and employed it to screen a small library of biologically active compounds with the aim of identifying potentially active molecular scaffolds (Figure 4a). Seven reported reaction buffers for NTH1 were tested with **GPE11** and **GPE15** to select optimal media conditions for screening (SI Figure S4). With the optimized buffer and probe conditions, **GPE15** (1 $\mu$M) was treated with 0.75 ng/$\mu$L hNTH1 pre-incubated with 20 $\mu$M of a small molecule for 30 min, then incubated for 6 h at 37°C. The activity of NTH1 was measured based on the ratio difference compared to that from identical compound+probe solutions lacking hNTH1, and the relative activity of NTH1 was determined by comparing

the activity upon the addition of each small molecule to the activity without any compound. This resulted in the preliminary identification of 51 hit compounds that lowered activity by at least 65% at 20 $\mu$M (Figure 4b).

The 51 hit compounds were then subjected to inspection for false-positives, which can arise from direct interaction of the compounds with the **GPE** probe or from inherent compound fluorescence (Figure 4c). The ratiometric nature of the probe enabled facile exclusion of false-positive candidates, leaving 19 compounds as eligible candidates (SI Figure S5). Further refinement was then carried out at lower concentrations to identify the most potent compounds of the set, resulting in three hit compounds that exhibited >65% inhibition at 5 $\mu$M.

These three hit compounds were evaluated with real-time NTH1 activity traces over a range of concentrations, and the most potent compound, NVP-AEW541, originally identified as an IGF-1R inhibitor,[34] showed submicromolar inhibitory activity with human NTH1 ($IC_{50}$ 0.78 $\mu$M) (Figure 4f, 4g, SI Figure S6). This inhibitory activity was further validated by MALDI-TOF analysis (SI Figure S11). NVP-AEW541 is a purine-like analogue, which is consistent with prior reports of purine analogs inhibiting the activity of glycosylases including OGG1, NTH1, and NEILs (Figure 4e).[16a] To our knowledge, the only previous report of a NTH1 inhibitor was as a secondary off-target activity of inhibitors of NEIL1 enzyme, and the compound showed an $IC_{50}$ > 20 $\mu$M for NTH1.[16a] Thus the new compound is more potent than prior inhibitors by over two orders of magnitude. To investigate the selectivity of this scaffold among DNA base excision repair enzymes, we used a published assay[16b] to evaluate its effects on several enzymes (SI Figure S8). The data show that NVP-AEW541 shows little or no inhibition of SMUG1, UNG, OGG1, MPG, and unedited NEIL1[35] at the highest concentration. Further experiments revealed that addition of NVP-AEW541 to HeLa cellular lysates in the presence of **GPE11np** probe reduced the excimer fluorescence enhancement, providing early evidence that NVP-AEW541 has efficacy in inhibiting the NTH1-directed repair of $^{5OH}U$ at the cellular lysate level (Figure 4h). The results provide a new and potent inhibitory scaffold for this enzyme target, and demonstrate the utility of the **GPE** probe design in measuring NTH1 activity. Further modification of the NVP-AEW541 scaffold should be possible to increase potency and selectivity of this new probe compound.

We have described a new probe design strategy for the direct detection of DNA glycosylase activity by utilizing pyrene excimer formation as a ratiometric reporter. In this strategy, a damaged base located between two pyrenes obstructs excimer formation, and the excision of the damaged base by a glycosylase restores long-wavelength excimer interactions. The design has been validated by developing DNA probes detecting NTH1 activity, for which no direct detection probe has previously been reported. The probe with $^{5OH}U$ between two pyrenes in the stem of an optimized hairpin structure shows robust fluorescence excimer:monomer ratio increases upon the addition of NTH1. A nuclease-protected version of probe (**GPE11np**) enabled the measurement of NTH1 activity at the cellular level, revealing that *nth1* knock-down HeLa cells have 30% lower $^{5OH}U$ excision activity than control HeLa cells, which implies that approximately 30% of $^{5OH}U$ excision is performed by NTH1. The probe was then applied for the screening of NTH1 inhibitors from a small

molecule library. False-positive candidates were effectively eliminated by taking the advantage of the ratiometric probe design, enabling the identification of the first potent and selective inhibitor scaffold for the enzyme (NVP-AEW541). Given the clinical importance of DNA repair activity, the **GPE** fluorescence probes, as well as new small molecule modulators that have been identified with the probes *in vitro*, are expected to have broad utility in the base excision repair field.

## Supplementary Material

Refer to Web version on PubMed Central for supplementary material.

## Acknowledgements

We thank the U.S. National Cancer Institute (CA217809 to ETK and CA090689 to SSD) for support.

## References

[1]. Williams SC, Parsons JL, Mol. Cell. Biol. 2018, 38, e00616–e00617. [PubMed: 29610152]

[2]. Lindahl T, Nature 1993, 362, 709–715. [PubMed: 8469282]

[3]. Golato T, Brenerman B, McNeill DR, Li J, Sobol RW, Wilson DM 3rd, Sci. Rep. 2017, 7, 13007–13019. [PubMed: 29021553]

[4]. Parsons JL, Dianov GL, DNA Repair 2013, 12, 326–333. [PubMed: 23473643]

[5]. Jacobs AL, Schar P, Chromosoma 2012, 121, 1–20. [PubMed: 22048164]

[6]. Bensu K, Barbara A. H, Nadja C. De S.-p., Vilhelm A. B, FASEB J. 2002, 16, 1895–1902. [PubMed: 12468454]

[7]. Shogo I, Tapan B, Rabindra R, Tadahide I, Istvan B, J. Biol. Chem. 1998, 273, 21585–21593. [PubMed: 9705289]

[8] a). Sandrine F, Thierry D, Jean-Luc R, Jean-Pierre P, Calogero T, Jean C, Chem. Res. Toxicol. 2000, 13, 1002–1010; [PubMed: 11080049] b)Alexandra V, Roger W, EMBO J. 2001, 20, 6520–6529. [PubMed: 11707422]

[9]. Yang N, Chaudhry MA, Wallace SS, DNA Repair 2006, 5, 43–51. [PubMed: 16111924]

[10]. Elder RH, Dianov GL, J. Biol. Chem. 2002, 277, 50487–50490. [PubMed: 12401779]

[11]. Trzeciak AR, Nyaga SG, Jaruga P, Lohani A, Dizdaroglu M, Evans MK, Carcinogenesis 2004, 25, 1359–1370. [PubMed: 15044326]

[12]. Goto M, Shinmura K, Igarashi H, Kobayashi M, Konno H, Yamada H, Iwaizumi M, Kageyama S, Tsuneyoshi T, Tsugane S, Sugimura H, Carcinogenesis 2009, 30, 1345–1352. [PubMed: 19414504]

[13]. Carter RJ, Parsons JL, Mol. Cell. Biol. 2016, 36, 1426–1437. [PubMed: 26976642]

[14]. Ryslava H, Doubnerova V, Kavan D, Vanek O, Proteomics J 2013, 92, 80–109.

[15]. Galick HA, Kathe S, Liu M, Robey-Bond S, Kidane D, Wallace SS, Sweasy JB, Proc. Natl. Acad. Sci. USA 2013, 110, 14314–14319. [PubMed: 23940330]

[16] a). Jacobs AC, Calkins MJ, Jadhav A, Dorjsuren D, Maloney D, Simeonov A, Jaruga P, Dizdaroglu M, McCullough AK, Lloyd RS, PLoS One 2013, 8, e81667; [PubMed: 24349107] b)Wilson DL, Kool ET, J. Am. Chem. Soc. 2019, 141, 19379–19388. [PubMed: 31774658]

[17]. Wilson DL, Kool ET, ACS Chem. Biol. 2018, 13, 1721–1733. [PubMed: 29156135]

[18] a). Jun YW, Wang T, Hwang S, Kim D, Ma D, Kim KH, Kim S, Jung J, Ahn KH, Angew. Chem. Int. Ed. 2018, 57, 10142–10147;b)Jun YW, Sarkar S, Singha S, Reo YJ, Kim HR, Kim JJ, Chang YT, Ahn KH, Chem. Commun. 2017, 53, 10800–10803.

[19]. Ren RX-F, Chaudhuri NC, Paris PL, IV SR, Kool ET, J. Am. Chem. Soc. 1996, 118, 7671–7678. [PubMed: 20865136]

[20] a). Winnik FM, Chem. Rev 1993, 93, 587–614;b)Gao J, Strassler C, Tahmassebi D, Kool ET, J. Am. Chem. Soc. 2002, 124, 11590–11591. [PubMed: 12296712]

[21]. Dou H, Mitra S, Hazra TK, J. Biol. Chem. 2003, 278, 49679–49684. [PubMed: 14522990]

[22] a). Satoko Y, Takuya U, Yoshiharu I, Kin-ichiro M, Kimitsuna W, Ichiro H, Nucleic Acids Res. 1994, 22, 2217–2221; [PubMed: 8036147] b)Edwards SK, Ono T, Wang S, Jiang W, Franzini RM, Jung JW, Chan KM, Kool ET, ChemBioChem 2015, 16, 1637–1646. [PubMed: 26073452]

[23] a). Smirnov S, Matray TJ, Kool ET, Santos C. d. l., Nucleic Acids Res. 2002, 30, 5561–5569; [PubMed: 12490724] b)Matray TJ, Kool ET, J. Am. Chem. Soc. 1998, 120, 6191–6192. [PubMed: 20852721]

[24]. Thiviyanathan V, Somasunderam A, Volk DE, Gorenstein DG, Chem. Commun. 2005, 400–402.

[25]. Hainke S, Singh I, Hemmings J, Seitz O, J. Org. Chem. 2007, 72, 8811–8819. [PubMed: 17941674]

[26] a). Beharry AA, Lacoste S, O'Connor TR, Kool ET, J. Am. Chem. Soc. 2016, 138, 3647–3650; [PubMed: 26967262] b)Wilson JN, Cho Y, Tan S, Cuppoletti A, Kool ET, Chembiochem 2008, 9, 279–285. [PubMed: 18072185]

[27]. Dizdaroglu M, Karahalil B, Senturker S, Buckley TJ, Roldan-Arjona T, Biochemistry 1999, 38, 243–246. [PubMed: 9890904]

[28] a). Choung S, Kim YJ, Kim S, Park HO, Choi YC, Biochem. Biophys. Res. Commun. 2006, 342, 919–927; [PubMed: 16598842] b)Squire Rumney I, Kool ET, J. Am. Chem. Soc 1995, 117, 5635–5646. [PubMed: 20871801]

[29]. Wilson DL, Beharry AA, Srivastava A, O'Connor TR, Kool ET, Angew. Chem. Int. Ed. 2018, 57, 12896–12900.

[30]. Takao M, Kanno S, Kobayashi K, Zhang QM, Yonei S, van der Horst GT, Yasui A, J. Biol. Chem. 2002, 277, 42205–42213. [PubMed: 12200441]

[31]. Saha T, Rih JK, Roy R, Ballal R, Rosen EM, J. Biol. Chem. 2010, 285, 19092–19105. [PubMed: 20185827]

[32] a). Bryant HE, Schultz N, Thomas HD, Parker KM, Flower D, Lopez E, Kyle S, Meuth M, Curtin NJ, Helleday T, Nature 2005, 434, 913–917; [PubMed: 15829966] b)Mendes-Pereira AM, Martin SA, Brough R, McCarthy A, Taylor JR, Kim JS, Waldman T, Lord CJ, Ashworth A, EMBO Mol. Med. 2009, 1, 315–322. [PubMed: 20049735]

[33]. Visnes T, Grube M, Hanna BMF, Benitez-Buelga C, Cazares-Korner A, Helleday T, DNA Repair 2018, 71, 118–126. [PubMed: 30228084]

[34]. Garcia-Echeverria C, Pearson MA, Marti A, Meyer T, Mestan J, Zimmermann J, Gao J, Brueggen J, Capraro H-G, Cozens R, Evans DB, Fabbro D, Furet P, Porta DG, Liebetanz J, Martiny-Baron G, Ruetz S, Hofmann F, Cancer Cell 2004, 5, 231–239. [PubMed: 15050915]

[35]. Yeo J, Goodman RA, Schirle NT, David SS, Beal PA, Proc. Natl. Acad. Sci. USA 2010, 107, 20715–20719. [PubMed: 21068368]

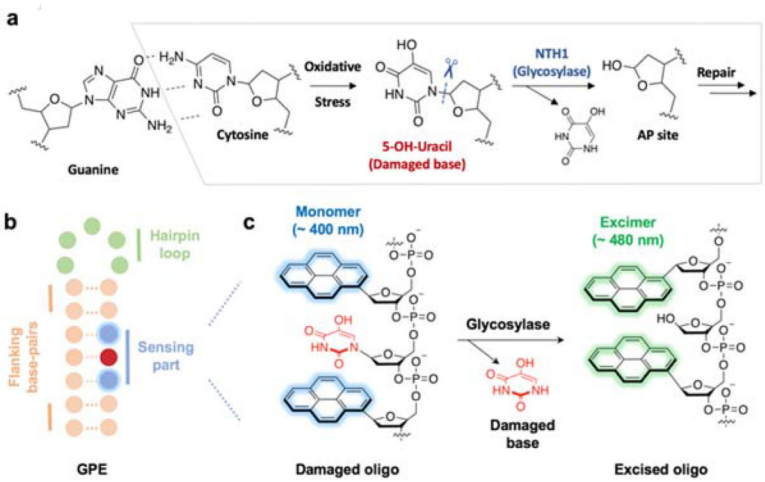


**Figure 1.**

a) Scheme showing pyrimidine damage in DNA by oxidation and its repair by NTH1. b) The design of a **GPE** DNA probe and c) illustration of the sensing part showing a “clamp” of pyrenes around the damaged base, yielding a change in fluorescence emission after enzymatic excision of the damage.

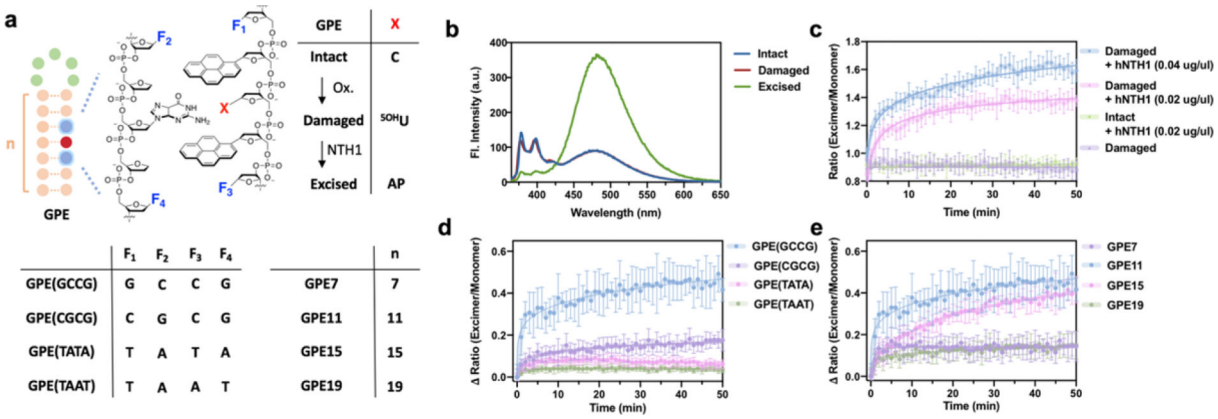


**Figure 2.**

a) The structure of the probe sensing module with different neighboring bases. b) Fluorescence spectra of **GPE_Intact** (blue), **GPE_Damaged** (red) and **GPE_Excised** (green). c) Fluorescence ratio change upon the addition of hNTH1. d) Fluorescence ratio change upon the addition of hNTH1 depending on varied neighboring bases. e) Stem length dependence of fluorescence ratio upon the addition of hNTH1. Fluorescence ratio was calculated based on the fluorescence intensity at 475 nm divided by the intensity at 400 nm with 350nm excitation. Conditions: 5 mM phosphate buffer (1 mM $MgCl_2$, 140 mM KCl, pH 7.4) with 0.02 $\mu$g/$\mu$L of hNTH1 at 37 $^{o}$C.

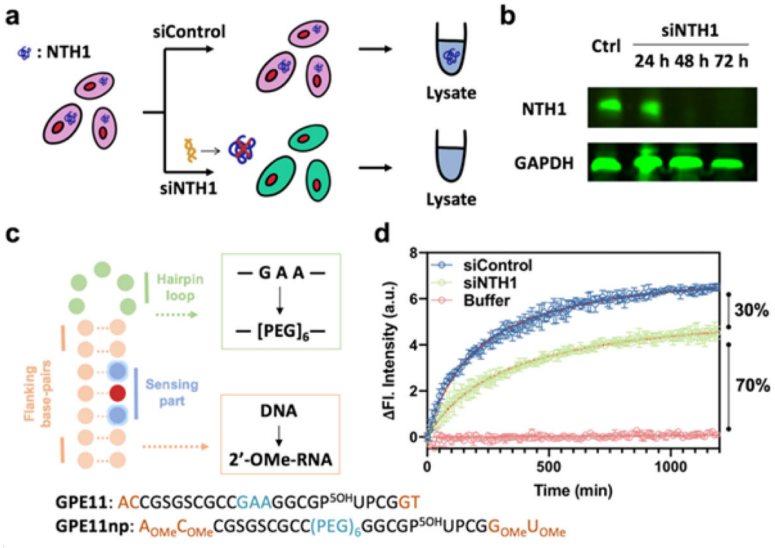


**Figure 3.**

a) Schematic showing preparation of NTH1 knock-down cellular lysate using siRNA directed to NTH1. b) Western blot results of siControl and siNTH1 incubated for 24, 48, and 72 h. c) Illustration showing probe modifications to confer nuclease resistance. d) The excimer fluorescence response of **GPE11np** upon the addition of cellular lysates. Experiments were carried out with 1 $\mu$M probe and HeLa lysate (0.12 $\mu$g/$\mu$L of total protein). Fluorescence signal was measured at 460 nm (355 nm excitation) over 20 h incubation at 37 $^{o}$C.

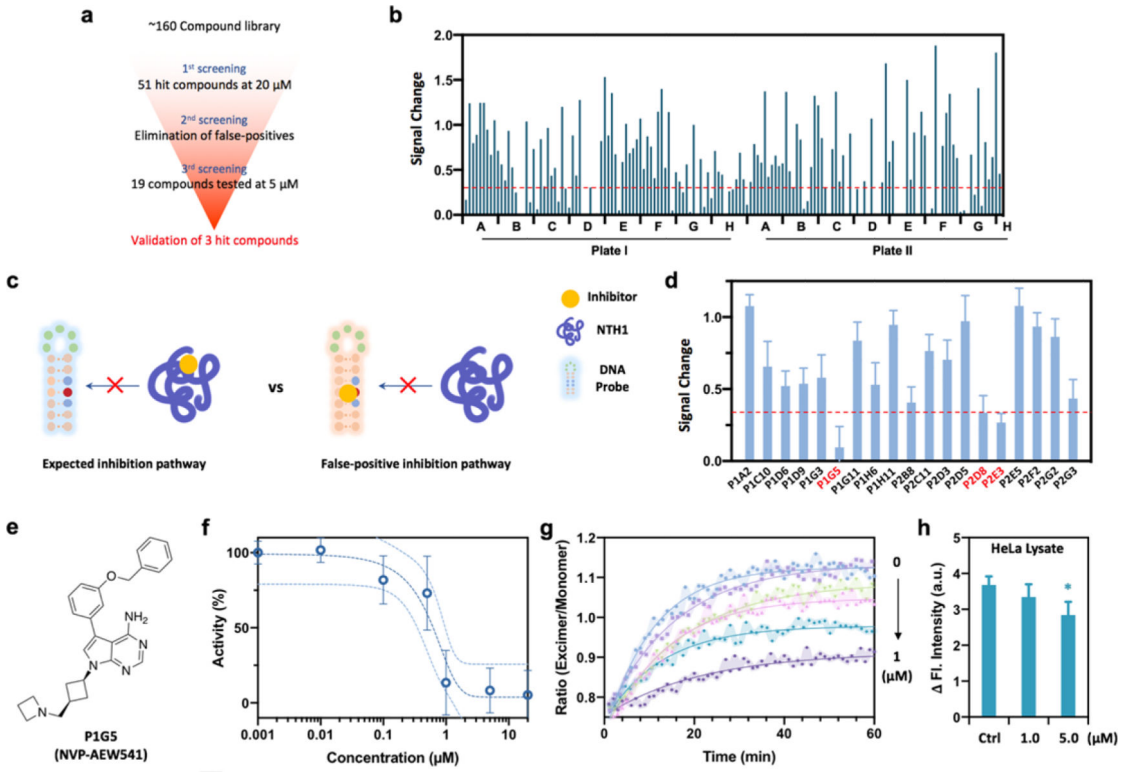


**Figure 4.**

(a) Flowchart of the screening process from a commercial small molecule library of 160 biologically active compounds. Chemical information on the library is given in Supporting Information. (b) Relative reactivity determined by **Δ**Ratio(Excimer/Monomer) in the first screening process. In this process, **GPE15** (1 $\mu$M) was treated with 0.75 ng/$\mu$L hNTH1 preincubated with 20 $\mu$M of each compound for 30 min. Threshold (relative reactivity = 0.3) in this screening is shown as a dashed line. (c) Illustration of expected inhibitory pathway and false-positive pathway that can result in fluorescence signals. (d) Relative reactivity in the third screening process. In this process, **GPE15** (1 $\mu$M) was treated with 0.75 ng/$\mu$L hNTH1 preincubated with 5 $\mu$M of each compound for 10 min. (e) Chemical structure of the hit compound. (f) Plot of activity of NTH1 with increasing NVP-AEW541 concentration. Three sigmoidal curves represent the average curve and the error range of the curve. (g) Real-time fluorescence traces of NTH1 activity with increasing concentrations of NVP-AEW541. (h) Comparison of fluorescence enhancement in cellular lysate upon the addition of varied concentrations of NVP-AEW541.